



Multichronometer thermochronologic modeling of migrating spreading ridge subduction in southern Patagonia

Andrea L. Stevens Goddard^{1,*} and Julie C. Fosdick²

¹Department of Geology, Rowan University, 201 Mullica Hill Road, Glassboro, New Jersey 08028, USA

²Department of Geosciences, University of Connecticut, 354 Mansfield Road, Storrs, Connecticut 06269, USA

ABSTRACT

The dynamic effects of spreading ridge subduction on the geology of the overriding plate have been used to account for changes in upper-plate topography, erosion rates and patterns, and regional stress regimes in Cordilleran systems. This study used an orogen-scale thermochronological modeling data set of 55 samples in the southern Patagonian Andes (47°S–54°S) to derive the spatio-temporal patterns of rock cooling relative to Miocene–present ridge subduction and slab window emplacement. These results identify a northward-migrating record of rock cooling and interpreted uplift from 20 Ma to 5 Ma throughout the arc batholith and retroarc that predate the subduction of the Chile Ridge spreading center by 2–5 m.y. We interpret this signal as the first orogen-scale evidence from Patagonia that rock uplift and erosion in ridge subduction settings are primarily driven by the generation of a thickened crustal welt along the leading edge of the obliquely subducting ridge. This signal is uniform across tectonic domains >160 km from the trench, indicating that ridge subduction does not trigger concentrated deformation only in the retroarc fold-and-thrust belt, as has been suggested. Moreover, rock cooling ceases within 10–20 m.y. of slab window emplacement, suggesting that asthenospheric upwelling and heating do not produce measurable thermal resetting in the upper crust above the slab window. Multiple thermochronometers are required to model the time-temperature histories that capture northward-migrating uplift and rock cooling associated with subduction of the Chile Ridge, a signal that is not evident from thermochronometric ages alone.

INTRODUCTION

Spreading ridge subduction is an important process in Cordilleran orogenesis (Thorkelson, 1996; Thorkelson et al., 2011) that causes large oceanic plates to break up into smaller plates and, depending on geometry and changing stress regimes, initiate new types of plate boundaries (Fig. 1A; Atwater and Stock, 1998). In contrast to the relatively well-understood effects of ridge subduction on magmatism, the structural, thermal, and dynamic effects on the overriding plate are more difficult to characterize, but they have critical implications for how we interpret tectonic and climatic histories from the geologic record. Modern and ancient slab windows along the Pacific Ocean Basin provide some examples of upper-plate modification. Along the San Andreas fault transform plate boundary (Fig. 1A), geodynamic and thermochronologic studies suggest that northward propagation of the Mendocino triple junction and trailing slab window (e.g., Liu et al.,

2012) formed a northward-migrating “crustal conveyor” of a thickened welt of lithosphere on the leading edge of the triple junction, followed by lithospheric thinning in the wake of triple junction passage (Furlong and Govers, 1999; Brady and Spotila, 2005). In the Alaska forearc basin, the asthenospheric window in the Yakutat/Pacific slab produces isostatic uplift of both the forearc region and arc plutons (Kortyna et al., 2013).

In the Patagonian Andes, the collision and northward migration of the Chile Ridge oceanic spreading center along the South American margin (Fig. 1) beginning in early Miocene time (Barckhausen et al., 2008; Breitsprecher and Thorkelson, 2009) were recorded by backarc adakitic volcanism (Ramos and Kay, 1992; Gorring et al., 2001; Kay et al., 2004). The modern location of the actively subducting ridge segment at 47°S is characterized by neotectonic activity, transtensional and transpressional deformation, and associated late Cenozoic rock cooling and exhumation (Thomson, 2002; Georgieva et al., 2016, 2019). Numerous workers have attempted

to recognize the local signature of the slab window in Patagonia from structural, thermochronologic, geomorphic, and sedimentary signals (e.g., Ramos, 2005; Haschke et al., 2006; Guillaume et al., 2013; Fosdick et al., 2013). However, these approaches have yet to fully show close spatio-temporal association with the older ridge segments. Thermochronometric studies in the region have consequently focused on other insightful observations from these data, including regional retroarc thrust belt deformation (Haschke et al., 2006; Fosdick et al., 2013; Guillaume et al., 2013) and late Cenozoic glacial erosion and climate variations (Thomson et al., 2010; Fosdick et al., 2013; Herman et al., 2013; Herman and Brandon, 2015; Christeleit et al., 2017).

In this study, we used thermal history modeling to read through overprinting signals of late Cenozoic climate-related erosion (Herman et al., 2013) and evaluate three potential mechanisms proposed for modification of upper-crustal geology in ridge subduction settings: (1) Increased coupling between the ridge and the overriding plate enhances or initiates retroarc shortening in the fold-and-thrust belt (Ramos, 2005; Haschke et al., 2006); (2) crustal heating from the upwelling asthenosphere through the slab window (Guillaume et al., 2010, 2013); and/or (3) isostatic uplift due to the formation of a crustal welt produced by lithospheric thickening and viscous flow along the leading edge of the obliquely subducting ridge, perpendicular to the trench and fold-and-thrust belt vergence (sensu lato Furlong and Govers, 1999). Although all three mechanisms may modify topography, deformational patterns, and/or the thermal regime of the upper crust, the predicted orogen-scale spatial and temporal patterns in the thermochronological record will be unique. For example, increased retroarc deformation may produce cratonward patterns of accelerated erosion and rock cooling in the fold-and-thrust belt during ridge subduction (e.g., Ramos, 2005; Haschke et al., 2006;

*E-mail: goddarda@rowan.edu

CITATION: Stevens Goddard, A.L., and Fosdick J.C., 2019, Multichronometer thermochronologic modeling of migrating spreading ridge subduction in southern Patagonia: *Geology*, <https://doi.org/10.1130/G46091.1>

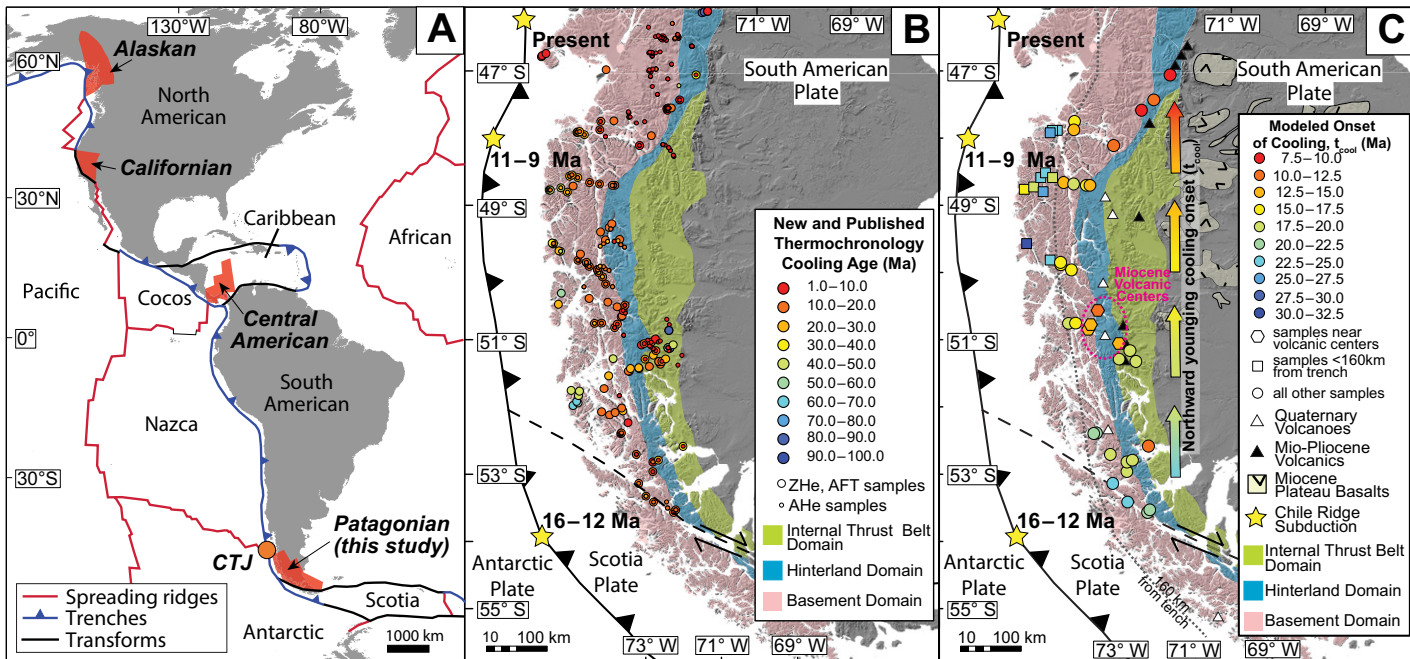


Figure 1. (A) Distribution of active spreading ridges and slab windows along North and South America Cordilleras (modified after Thorkelson et al., 2011). CTJ—Chile triple junction. (B) New and published (U - Th)/He (ZHe), apatite fission-track (AFT), and apatite (U - Th)/He (AHe) ages plotted on simplified tectonic map of southern Patagonian Andes (Thomson et al., 2001, 2010; Haschke et al., 2006; Fosdick et al., 2013; Guillaume et al., 2013; Georgieva et al., 2016; Christeleit et al., 2017). Locations and ages of spreading ridge subduction are shown along trench with yellow stars (after Breitsprecher and Thorkelson, 2009). (C) Dates of onset of cooling, t_{cool} , determined by thermal modeling results. Neogene retroarc volcanic activity between 47° S and 54° S is modified after Ramírez de Arellano (2012).

Fosdick et al., 2013), whereas upwelling hot asthenosphere through the trailing slab window has been proposed to transfer heat to the upper crust after the passage of the ridge (e.g., Guillaume et al., 2013). Alternatively, trench-perpendicular shortening and crustal thickening along the leading edge of the obliquely subducting ridge will precede ridge subduction, producing a migrating wave of isostatic rock uplift and interpreted erosion (Furlong and Govers, 1999; Brady and Spotila, 2005; Peng et al., 2017).

METHODS AND RESULTS

Inverse thermal history modeling of published (52) and new (3) samples was conducted for samples spanning the basement, hinterland, and internal thrust belt domains of the southern Patagonian Andes between 47° S and 54° S (Thomson et al., 2001, 2010; Fosdick et al., 2013). Methods outlining sample collection and analysis of new data are included in the GSA Data Repository¹. Samples were selected from all published studies (Fig. 1A) for inverse thermal history modeling based on the existence of multichronometer data for each sample from at least two of the zircon (U - Th)/He (ZHe), apatite fission-track (AFT), and apatite (U - Th)/He (AHe) systems sensitive

to a bulk closure temperature of ~ 200 – 50 °C (Reiners et al., 2004; Guenther et al., 2013), 140–90 °C (Green et al., 1989; Ketcham et al., 2007), and ~ 110 –65 °C, respectively (Farley, 2000; Flowers et al., 2009), depending primarily on radiation damage in the crystal, cooling rate, mineral chemistry, and grain size. Fifty-five samples met these criteria and were modeled using the inverse modeling application in HeFTy v. 1.9.3 (Ketcham, 2005). For each modeled sample, we included all available single-grain ZHe, AFT, and AHe data to evaluate a large ($>100,000$) set of time-temperature (t - T) histories and identify those permissible by the thermochronometric data. Model constraints for the 100–0 Ma time period were left broad to explore all cooling histories, with constraints only at model initiation (100 °C and 300 °C between 80 and 50 Ma), consistent with evidence from regional geology (Calderón et al., 2016) and modern surface temperatures of 10 ± 5 °C. HeFTy inversions were required to run until 100 t - T paths were identified with a goodness of fit >0.5 .

The HeFTy inverse modeling routine identified 100 good-fit paths for 45 of the 55 samples with multimethod data, including existing models published in Fosdick et al. (2013). For 10 samples, HeFTy's exploration of $>100,000$ possible t - T paths failed to identify any good-fit paths, potentially owing to a nongeologic discrepancy between thermochronometric data, and these samples were excluded from further analysis. Our results captured t - T histories with pro-

nounced inflection points that marked a period of accelerated cooling in the Miocene observed in t - T results from the batholith, hinterland, and internal thrust belt domains for all but one sample between 47° S and 54° S (Fig. 2). For each modeled sample, we coded the timing of each inflection point (t_{cool}), signifying the onset of modeled cooling (Fig. DR2). The temporal range of each t_{cool} point (shown by error bars) represents the plausible modeled inflection point as accepted by the measured thermochronometric data. Model results and parameters for extracting the onset of cooling are included in the Data Repository.

The new onset of cooling (t_{cool}) data set from model output shows that, although 44 of 45 modeled samples yielded accelerated Miocene cooling, the timing of this inflection in t - T paths is systematically variable among samples, ranging between ca. 19 and 6 Ma (Table DR2). The age of onset of cooling decreases northward along the Patagonian Andes from 54° S to 47° S (Fig. 2B). Twenty-nine of the 45 modeled samples identified a second change in cooling rates, a deceleration of cooling that followed within 10 m.y. of acceleration, but this trend does not systematically vary by latitude. Additionally, we observed a positive relationship between t_{cool} and distance from the trench (Fig. DR1). Nine of eleven samples located <160 km from the trench preserve t - T histories that do not identify cooling 2–5 m.y. before ridge migration and instead preserve an earlier onset of t_{cool} (Figs. 1C and 2B). We also documented a

¹GSA Data Repository item 2019203, extended analytical and modeling methods, new data measurements, and archives of all thermal history models used in the study, is available online at <http://www.geosociety.org/datarerepository/2019/>, or on request from editing@geosociety.org.

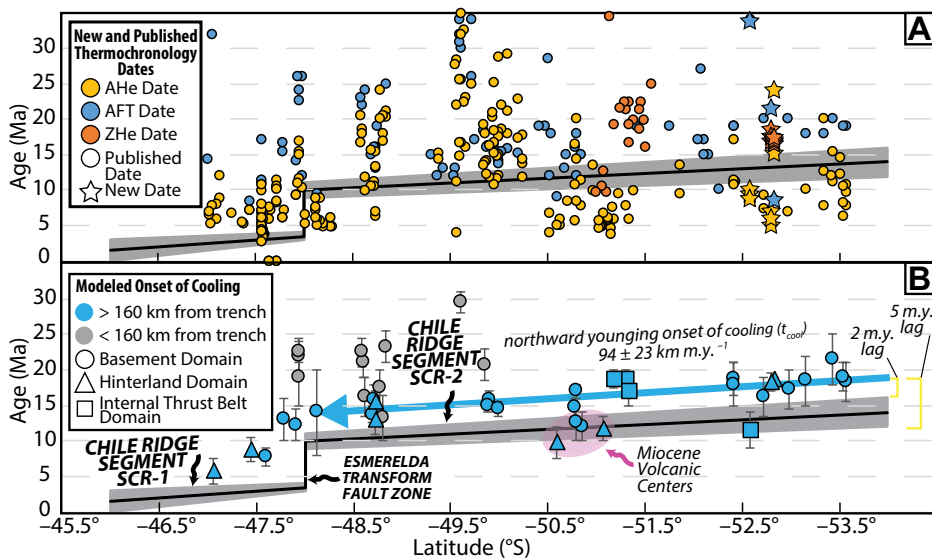


Figure 2. Location of subduction of Chile Ridge segments SCR-1 and SCR-2 as well as Esmerelda transform fault zone are plotted by latitude based on reconstructions by Breitsprecher and Thorkelson (2009). (A) Compilation of new and published (U-Th)/He (ZHe), apatite fission-track (AFT), and apatite (U-Th)/He (AHe) thermochronology dates from all tectonic domains between 47°S and 54°S. (B) Dates of onset of cooling, t_{cool} , across all tectonic domains as determined by thermochronological modeling in this study plotted by latitude. Error bars reflect range of acceptable modeled t_{cool} as constrained by thermochronology data.

departure from the northward-younging trend near localized Miocene magmatic centers near 51°S (Ramírez de Arellano et al., 2012), where the thermal record of t_{cool} was overprinted by younger magmatism (Fosdick et al., 2013). We emphasize that recognition of these spatially and temporally controlled cooling signals may not be reflected by any or all of the reported ZHe, AFT, or AHe ages alone (Fig. 2A) and requires systematic modeling to resolve complete thermal histories over this time period.

ONSET OF NEOGENE COOLING AND NORTHWARD MIGRATION OF CHILE RIDGE SUBDUCTION

The modeled onset of cooling shows a northward younging of t_{cool} that predated subduction of the Chile Ridge segment SCR-2 between ca. 16 and 10 Ma by 2–5 m.y. and was synchronous across all tectonic domains (Fig. 2B; Breitsprecher and Thorkelson, 2009). A linear regression of t_{cool} observations above the Chile Ridge segment SCR-2 and >160 km from the trench suggests that the onset of cooling migrated north along the subduction zone at a rate of 94 ± 23 km m.y.⁻¹, a rate within error of kinematic reconstructions of Chile Ridge subduction migration (Fig. 2B; Breitsprecher and Thorkelson, 2009). The subsequent subduction of the Esmerelda transform fracture zone (ca. 10 Ma) corresponds to a hiatus in the propagation of regional cooling that resumed 2–5 m.y. prior to subduction of the Chile Ridge (segment SCR-1) at ca. 4 Ma. The synchronicity between the northward migration of t_{cool} and the kinematic reconstructions of ridge subduction 2–5 m.y. later provides the first evi-

dence of an orogen-scale response to ridge subduction in Patagonia. We propose that orogen-parallel crustal thickening and welt development along the leading edge of the subducting ridge was the primary mechanism for regional rock uplift and associated erosion-driven cooling in Patagonia and other ridge subduction settings (Furlong and Govers, 1999). Both numerical models and geochemical data suggest that slabs have an effective edge that extends beyond the geometrically defined slab edge used in kinematic reconstructions (Groome and Thorkelson, 2009; Thorkelson et al., 2011). Deformation along this more extended effective edge may help to explain the earlier development of lithospheric thickening before subduction of the geometrically defined ridge edge. In Figure 3, we present a conceptual model in which shortening parallel to the leading edge of the subducted Chile Ridge produces a thickened crustal welt. Enhanced erosion of this feature is consistent with the northward-younging t_{cool} points derived in this study using thermal models. In 29 of 45 model results, cooling slowed within 10 m.y. of the onset of cooling (Table DR2), suggesting that asthenospheric upwelling through the slab window did not significantly contribute to a thermochronometric signature via thermal reheating of the upper crust during the 10–20 m.y. following slab window emplacement, consistent with recent observations near the triple junction (Georgieva et al., 2019).

The absence of a systematically northward-migrating t_{cool} in samples located <160 km from the trench could be controlled by local variations in the structural regime, as all of these samples

came from locations in and around the Campana Archipelago (Fig. 1). Alternatively, it is possible that the absence of the cooling signal close to the trench defines an important thermo-mechanical threshold that governs the development of regional topography during ridge subduction. If the latter case is true, a higher magnitude of rock uplift farther inboard may be an important signature of regional rock uplift and cooling due to ridge subduction.

CONCLUSIONS

This study identified an orogen-scale cooling signature of spreading ridge subduction along the leading edge of the subducting Chile Ridge. In Patagonia, this deformation generated a thickened crustal welt that correlates closely with the development of topography 2–5 m.y. prior to passage of the subducting spreading ridge. We identified this phenomenon in the thermochronological record as cooling produced from enhanced erosion across tectonic domains >160 km from the trench. Although heat generated from asthenospheric upwelling through the slab window may increase heat flow at depth (Thorkelson, et al., 2011), we found no thermochronometric evidence for reheating or thermal uplift–driven erosion and cooling within 10–20 m.y. of slab window formation. Detecting the subduction of the Chile Ridge and its impact on Cordilleran processes requires highly integrated thermal history models from an array of thermochronometers to elucidate the t - T history of rocks across tectonic domains.

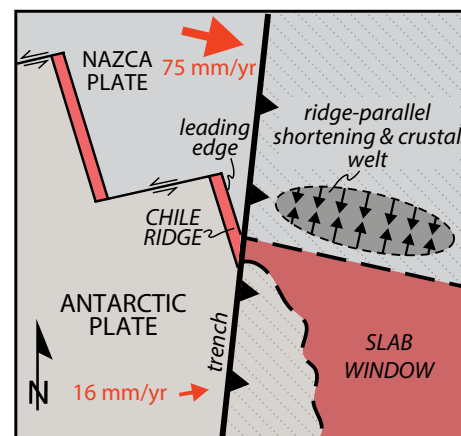


Figure 3. Schematic diagram of spreading ridge subduction in southern Patagonia. Map view is shown with overriding continental South American plate removed above slab window. Oblique subduction of spreading ridge produces ridge-parallel shortening in advance of leading edge of subducted ridge and development of crustal welt. Erosion of this topographic welt drives cooling signature observed in our thermochronologic modeling. Slab window forms inboard of trailing ridge edge due to difference in convergence rates between Nazca plate and Antarctic plate (Breitsprecher and Thorkelson, 2009).

ACKNOWLEDGMENTS

Postdoctoral research funding in support of this work was provided to A. Stevens Goddard by the University of Connecticut. We are indebted to M. Calderón for conversations on Patagonian geology and logistical support. V. Astarte Muller, M. Ghiglione, C. Ramírez de Arellano, D. Rojo, F. Torres, and the crew of the *Marypaz II* provided excellent field assistance through FONDECYT grant 1161818. We thank S. Thomson at the Arizona Fission Track Laboratory for assistance with apatite fission-track analysis and discussions about the exhumation history of Patagonia. (U-Th)/He thermochronology analyses were performed at the University of Colorado Thermochronology Research and Instrumentation Laboratory (CU TRaIL). We appreciate feedback on early drafts of this manuscript by Jay Chapman and Marty Grove and reviews by Kendra Murray and two anonymous reviewers.

REFERENCES CITED

Atwater, T., and Stock, J., 1998, Pacific–North America plate tectonics of the Neogene southwestern United States: An update: *International Geology Review*, v. 40, p. 375–402, <https://doi.org/10.1080/00206819809465216>.

Barckhausen, U., Ranero, C.R., Cande, S.C., Engels, M., and Weinrebe, W., 2008, Birth of an intraoceanic spreading center: *Geology*, v. 36, p. 767–770, <https://doi.org/10.1130/G25056A.1>.

Brady, R.J., and Spotila, J., 2005, Southward-younging apatite (U-Th)/He ages in the northern California Coast Ranges due to a northward-migrating crustal welt: *Earth and Planetary Science Letters*, v. 235, p. 107–122, <https://doi.org/10.1016/j.epsl.2005.03.010>.

Breitsprecher, K., and Thorkelson, D.J., 2009, Neogene kinematic history of Nazca–Antarctic–Phoenix slab windows beneath Patagonia and the Antarctic Peninsula: *Tectonophysics*, v. 464, p. 10–20, <https://doi.org/10.1016/j.tecto.2008.02.013>.

Calderón, M., Francisco Hervé, F., Francisco Fuentes, F., and Fosdick, J.C., 2016, Tectonic evolution of Paleozoic and Mesozoic Andean metamorphic complexes and the Rocas Verdes ophiolites in southern Patagonia, in Ghiglione, M., ed., *Geodynamic Evolution of the Southernmost Andes*: Berlin, Springer-Verlag, p. 7–36, https://doi.org/10.1007/978-3-319-39727-6_2.

Christeleit, E.C., Brandon, M.T., and Shuster, D.L., 2017, Miocene development of alpine glacial relief in the Patagonian Andes, as revealed by low-temperature thermochronometry: *Earth and Planetary Science Letters*, v. 460, p. 152–163, <https://doi.org/10.1016/j.epsl.2016.12.019>.

Farley, K.A., 2000, Helium diffusion from apatite: General behavior as illustrated by Durango fluorapatite: *Journal of Geophysical Research*, v. 105, p. 2903–2914, <https://doi.org/10.1029/1999JB900348>.

Flowers, R.M., Ketcham, R.A., Shuster, D.L., and Farley, K.A., 2009, Apatite (U-Th)/He thermochronometry using a radiation damage accumulation and annealing model: *Geochimica et Cosmochimica Acta*, v. 73, p. 2347–2365, <https://doi.org/10.1016/j.gca.2009.01.015>.

Fosdick, J.C., Grove, M., Hourigan, J.K., and Calderón, M., 2013, Retroarc deformation and exhumation near the end of the Andes, southern Patagonia: *Earth and Planetary Science Letters*, v. 361, p. 504–517, <https://doi.org/10.1016/j.epsl.2012.12.007>.

Furlong, K.P., and Govers, R., 1999, Ephemeral crustal thickening at a triple junction: The Mendocino crustal conveyor: *Geology*, v. 27, p. 127–130, [https://doi.org/10.1130/0091-7613\(1999\)027<127:ECTAAT>2.3.CO;2](https://doi.org/10.1130/0091-7613(1999)027<127:ECTAAT>2.3.CO;2).

Georgieva, V., Melnick, D., Schildgen, T.F., Ehlers, T.A., Lagabrielle, Y., Enkelmann, E., and Strecker, M.R., 2016, Tectonic control on rock uplift, exhumation, and topography above an oceanic ridge collision: Southern Patagonian Andes (47°S), Chile: *Tectonics*, v. 35, p. 1317–1341, <https://doi.org/10.1002/2016TC004120>.

Georgieva, V., Gallagher, K., Sobczyk, A., Sobel, E.R., Schildgen, T.F., Ehlers, T.A., and Strecker, M.R., 2019, Effects of slab-window, alkaline volcanism, and glaciation on thermochronometer cooling histories, Patagonian Andes: *Earth and Planetary Science Letters*, v. 511, p. 164–176.

Gorring, M.L., Gorring, M.L., Kay, S.M., and Kay, S.M., 2001, Mantle processes and sources of Neogene slab window magmas from southern Patagonia, Argentina: *Journal of Petrology*, v. 42, p. 1067–1094, <https://doi.org/10.1093/petrology/42.6.1067>.

Green, P.F., Duddy, I.R., Laslett, G.M., Hegarty, K.A., Gleadow, A.J.W., and Lovering, J.F., 1989, Thermal annealing of fission tracks in apatite: 4. Quantitative modeling techniques and extension to geological time scales: *Chemical Geology*, v. 79, p. 155–182.

Groome, W.G., and Thorkelson, D.J., 2009, The three-dimensional thermo-mechanical signature of ridge subduction and slab window migration: *Tectonophysics*, v. 464, p. 70–83, <https://doi.org/10.1016/j.tecto.2008.07.003>.

Guillaume, B., Moroni, M., Funiciello, F., Martinod, J., and Faccenna, C., 2010, Mantle flow and dynamic topography associated with slab window opening: Insights from laboratory models: *Tectonophysics*, v. 496, p. 83–98, <https://doi.org/10.1016/j.tecto.2010.10.014>.

Guenther, W.R., Reiners, P.W., Ketcham, R.A., Nasdala, L., and Giester, G., 2013, Helium diffusion in natural zircon: radiation damage, anisotropy, and the interpretation of zircon (U-Th)/He thermochronology: *American Journal of Science*, v. 313, p. 145–198, <https://doi.org/10.2475/03.2013.01>.

Guillaume, B., Gautheron, C., Simon-Labrec, T., Martinod, J., Roddaz, M., and Douville, E., 2013, Dynamic topography control on Patagonian relief evolution as inferred from low temperature thermochronology: *Earth and Planetary Science Letters*, v. 364, p. 157–167, <https://doi.org/10.1016/j.epsl.2012.12.036>.

Haschke, M., Sobel, E.R., Blisniuk, P., Strecker, M.R., and Warkus, F., 2006, Continental response to active ridge subduction: *Geophysical Research Letters*, v. 33, L15315, <https://doi.org/10.1029/2006GL025972>.

Herman, F., and Brandon, M., 2015, Mid-latitude glacial erosion hotspot related to equatorial shifts in southern Westerlies: *Geology*, v. 43, p. 987–990, <https://doi.org/10.1130/G37008.1>.

Herman, F., Seward, D., Valla, P.G., Carter, A., Kohn, B., Willett, S.D., and Ehlers, T.A., 2013, Worldwide acceleration of mountain erosion under a cooling climate: *Nature*, v. 504, p. 423–426, <https://doi.org/10.1038/nature12877>.

Kay, S.M., Gorring, M., and Ramos, V.A., 2004, Magmatic sources, setting and causes of Eocene to Recent Patagonian plateau magmatism (36°S to 52°S latitude): *Revista de la Asociación Geológica Argentina*, v. 59, p. 556–568.

Ketcham, R.A., 2005, Forward and inverse modeling of low-temperature thermochronometry data: *Reviews in Mineralogy and Geochemistry*, v. 58, p. 275–314, <https://doi.org/10.2138/rmg.2005.58.11>.

Ketcham, R.A., Carter, A., Donelick, R.A., Barbarand, J., and Hurford, A.J., 2007, Improved modeling of fission-track annealing in apatite: *The American Mineralogist*, v. 92, p. 799–810, <https://doi.org/10.2138/am.2007.2281>.

Kortyna, C., Donaghay, E., Trop, J.M., and Idleman, B., 2013, Integrated provenance record of a forearc basin modified by slab-window magmatism: Detrital-zircon geochronology and sandstone compositions of the Paleogene Arkose Ridge Formation, south-central Alaska: *Basin Research*, v. 26, p. 436–460, <https://doi.org/10.1111/bre.12033>.

Liu, K., Levander, A., Zhai, Y., Porritt, R.W., and Allen, R.M., 2012, Asthenospheric flow and lithospheric evolution near the Mendocino triple junction: *Earth and Planetary Science Letters*, v. 323–324, p. 60–71, <https://doi.org/10.1016/j.epsl.2012.01.020>.

Peng, Y., Dong, D., Yan, J., and Chen, W., 2017, Geodetic constraint on the motion of a slab window: Implication for the Mendocino crustal conveyor model: *Geophysical Research Letters*, v. 44, p. 7187–7193, <https://doi.org/10.1002/2017GL074149>.

Ramírez de Arellano, C., Putlitz, B., Müntener, O., and Ovtcharova, M., 2012, High precision U/Pb zircon dating of the Chaltén plutonic complex (Cerro Fitz Roy, Patagonia) and its relationship to arc migration in the southernmost Andes: *Tectonics*, v. 31, TC4009, <https://doi.org/10.1029/2011TC003048>.

Ramos, V.A., 2005, Seismic ridge subduction and topography: Foreland deformation in the Patagonian Andes: *Tectonophysics*, v. 399, p. 73–86, <https://doi.org/10.1016/j.tecto.2004.12.016>.

Ramos, V.A., and Kay, S.M., 1992, Southern Patagonian plateau basalts and deformation: Backarc testimony of ridge collisions: *Tectonophysics*, v. 205, p. 261–282, [https://doi.org/10.1016/0040-1951\(92\)90430-E](https://doi.org/10.1016/0040-1951(92)90430-E).

Reiners, P.W., Spell, T.L., Nicolescu, S., and Zanetti, K.A., 2004, Zircon (U-Th)/He thermochronometry: He diffusion and comparisons with $^{40}\text{Ar}/^{39}\text{Ar}$ dating: *Geochimica et Cosmochimica Acta*, v. 68, p. 1857–1887, <https://doi.org/10.1016/j.gca.2003.10.021>.

Thomson, S.N., 2002, Late Cenozoic geomorphic and tectonic evolution of the Patagonian Andes between latitudes 42°S and 46°S: An appraisal based on fission-track results from the transpessional intra-arc Liquiñe–Ofqui fault zone: *Geological Society of America Bulletin*, v. 114, p. 1159–1173.

Thomson, S.N., Hervé, F., and Stöckhert, B., 2001, Mesozoic–Cenozoic denudation history of the Patagonian Andes (southern Chile) and its correlation to different subduction processes: *Tectonics*, v. 20, p. 693–711, <https://doi.org/10.1029/2001TC000013>.

Thomson, S.N., Brandon, M.T., Tomkin, J.H., Reiners, P.W., Vásquez, C., and Wilson, N.J., 2010, Glaciation as a destructive and constructive control on mountain building: *Nature*, v. 467, p. 313–317, <https://doi.org/10.1038/nature09365>.

Thorkelson, D.J., 1996, Subduction of diverging plates and the principles of slab window formation: *Tectonophysics*, v. 255, p. 47–63, [https://doi.org/10.1016/0040-1951\(95\)00106-9](https://doi.org/10.1016/0040-1951(95)00106-9).

Thorkelson, D.J., Madsen, J.K., and Sluggett, C.L., 2011, Mantle flow through the Northern Cordilleran slab window revealed by volcanic geochemistry: *Geology*, v. 39, p. 267–270, <https://doi.org/10.1130/G31522.1>.

Printed in USA